Conduction of surface electrons in a topological insulator with spatially random magnetization

S. Kudła,[1] A. Dyrdał,[2,3] V. K. Dugaev,[1] J. Berakdar,[2] and J. Barnaś[3,4]

[1]*Department of Physics and Medical Engineering, Rzeszów University of Technology, Al. Powstańców Warszawy 6, 35-959 Rzeszów, Poland*

[2]*Institute of Physics, Martin-Luther Universität Halle-Wittenberg, 06099 Halle (Saale), Germany*

[3]*Faculty of Physics, Adam Mickiewicz University in Poznań, ul. Uniwersytetu Poznańskiego 2, 61-614 Poznań, Poland*

[4]*Institute of Molecular Physics, Polish Academy of Sciences, ul. M. Smoluchowskiego 17, 60-179 Poznań, Poland*

(Received 6 June 2019; published 27 November 2019)

Using the Green functions method we study the transport properties of surface electrons of topological insulators in the presence of a correlated random exchange field. Such an exchange field may be induced by a random magnetization with correlated fluctuations. We determine the relaxation times due to scattering from the magnetization fluctuations and also from randomly distributed scalar impurities. The longitudinal charge conductivity is evaluated and discussed while accounting for vertex corrections.

DOI: 10.1103/PhysRevB.100.205428

I. INTRODUCTION

Topological properties of matter are currently at the front line of research in condensed matter physics [1,2]. Much attention has been focused recently on surface states in topological insulators (TIs), where electrons at the surface behave as massless Dirac fermions with spin-momentum locking [3–5]. This spin locking leads to novel spin-dependent transport phenomena [6–12].

It is known that owing to the proximity-induced exchange interaction, a thin ferromagnetic layer deposited on the surface of a TI opens a gap at the Dirac point in the electronic spectrum [13–15]. Generally, the proximity-induced exchange field not only affects the spectrum of electronic surface states, but the accompanied magnetic disorder at the interface also modifies relaxation processes of surface electrons in TIs and hence their spin-dependent transport properties. Indeed, the impact of magnetic disorder on transport properties of TIs has already been addressed [16]. It is also worth to note that hybrid systems based on TIs and thin ferromagnetic films, or on TIs with surfaces that are intentionally decorated by magnetic adatoms, bear great potential for spin-to-charge conversion phenomena [17–19].

The main objective of this paper is the description of the impact of magnetic disorder at the surface of a TI on its transport properties. It is well known that magnetic disorder may have different sources. For instance, the intrinsic magnetic properties of amorphous alloys such as local magnetization, magnetocrystalline and exchange energies, etc., fluctuate in space due to a random distribution of magnetic ions (as a consequence of external and internal stresses) [20–22]. Spatially random magnetic fields may also be realized in semiconductor heterostructures leading to interesting magnetotransport phenomena, including negative magnetoresistance due to weak localization, positive magnetoresistance related to small angle scattering of ballistic electrons by flux tubes, or the presence of extended states analogous to quantum Hall edge states in random magnetic fields with zero average value. Random magnetic fields in 2DEG heterostructures are realized, e.g., by capping the sample with a superconducting film that ensures inhomogeneous distribution of magnetic flux tubes when an external magnetic field is applied (see, e.g., Refs. [23–26]). Another possibility is to place a rough demagnetized permanent magnet (such as NdFeB) on top of the heterostructure surface with two-dimensional (2D) electron gas [27,28].

According to the above, one may also expect a number of transport phenomena induced by magnetic disorder at the surface of TIs, 2D graphenelike crystals, and quantum-Hall systems [29–32]. For instance, it was shown that the presence of magnetic impurities at the surface of TIs may lead to a planar Hall effect as well as to the in-plane magnetoresistance which is a mixture of the anisotropic and spin magnetoresistance [29]. Moreover, random magnetic impurities may lead to an opening of an energy gap for the edge states [33–35], and also may improve the quality of the quantum anomalous Hall effect in magnetic TIs [36]. Recently, the electron states at the surface of a TI attached to a ferromagnet described by the XY model have also been considered, and it was shown that the classical magnetic fluctuations in the ferromagnet could be mapped onto the problem of Dirac fermions in a random magnetic field [37].

Here we consider a model system where the spatially fluctuating magnetization interacts with the surface electrons in TIs due to an exchange field. We assume that the average value of the magnetization (or the exchange field) vanishes. However, $\langle M(\mathbf{r})M(\mathbf{r}')\rangle$ is finite and is described by a given correlation function $\langle M(\mathbf{r})M(\mathbf{r}')\rangle = \mathcal{C}(\mathbf{r}-\mathbf{r}')$. One should note that the problem of a random-mass term, as it appears in the presence of a spatially fluctuating magnetization, has been discussed for instance in Refs. [30–32], where the problem of a spatially fluctuating gap in the Dirac model has been considered in the context of integer quantum Hall effect [32] and electronic transport in graphene [30,31]. In these works the authors used white-noise Gaussian disorder. Here we consider a 2D Dirac model with a correlated mass disorder, which we relate to magnetization correlations on top of the topological insulator. As we show, the choice of correlation function, characterized by correlation length, is crucial for the

dependence of electron relaxation on energy and, correspondingly, for the dependence of resistance on temperature. The model is described in Sec. II. In Secs. III and IV we show that magnetic fluctuations have a significant impact on the relaxation time and transport properties of surface electrons in TIs. Summary and final conclusions are in Sec. V.

II. MODEL

We consider 2D electrons at the surface of a topological insulator in a random magnetization field (equivalently, in a random exchange field). The system is described by the following single particle Hamiltonian:

$$\hat{H} = -iv\boldsymbol{\sigma}\cdot\nabla + \hat{V}, \tag{1}$$

where $v = \hbar v_F$ and v_F is the electron (Fermi) velocity, while $\boldsymbol{\sigma} = (\sigma_x, \sigma_y, \sigma_z)$ is the vector of the Pauli matrices operating in the spin space. The scattering potential $\hat{V}$ describes the spatial fluctuations of the random magnetization (exchange) field $M(\mathbf{r})$, and also includes the scattering potential from random impurities,

$$\hat{V} = M(\mathbf{r})\,\sigma_z + V_0(\mathbf{r})\,\sigma_0. \tag{2}$$

Here $M(\mathbf{r})$ is measured in energy units and is Gaussian distributed, meaning that $M(\mathbf{r})$ vanishes on average, $\langle M(\mathbf{r})\rangle = 0$, but the second statistical moment is finite and is given in the form $\langle M(\mathbf{r})\,M(\mathbf{r}')\rangle = \mathcal{C}(\mathbf{r}-\mathbf{r}') = \langle M^2\rangle\, g(|\mathbf{r}-\mathbf{r}'|)$. All higher even-order statistical moments reduce to the second-order one, whereas the odd-order correlators vanish. The correlation function $g(|\mathbf{r}-\mathbf{r}'|)$ is governed by the characteristic correlation length ξ of the fluctuations [38,39]. The Fourier transform of $\mathcal{C}(\mathbf{r}-\mathbf{r}')$ has the Gaussian form $C(\mathbf{q}) = \langle M^2\rangle\xi^2 e^{-q^2\xi^2}$. The second term in Eq. (2), $V_0(\mathbf{r})\sigma_0$, is the scattering potential due to randomly distributed impurities. We assume isotropic pointlike scalar potential of the impurities, $V_0(\mathbf{r}) = \sum_i V^i\delta(\mathbf{r}-\mathbf{R}_i)$ ($\mathbf{R}_i$ indicates the random positions of impurities), which vanishes on average, $\langle V^i\rangle = 0$, and only the second statistical cumulant is finite, $\langle (V^i)^2\rangle = V_0^2 \neq 0$. Thus, for the scalar part of the scattering potential we consider the white-noise distribution $\langle |V_{0\,\mathbf{k}\mathbf{k}'}|^2\rangle = n_i V_0^2$, where n_i is the concentration of impurities.

In the following calculations, the influence of the random magnetization and random impurities on the transport properties is treated perturbatively. The retarded Green function corresponding to the unperturbed Hamiltonian reads

$$G^{0R}(\varepsilon,\mathbf{k}) = \frac{\varepsilon + v\boldsymbol{\sigma}\cdot\mathbf{k}}{(\varepsilon-\varepsilon_{1k}+i\delta)(\varepsilon-\varepsilon_{2k}+i\delta)}, \tag{3}$$

where $\varepsilon_{1,2k} = \pm vk \equiv \pm\varepsilon_k$ are the eigenvalues of the unperturbed part of the Hamiltonian (1). In the following we show explicitly how scattering on random magnetization and random impurities affects the relaxation time and the conductivity of the surface electrons in TIs.

III. SELF-ENERGY AND RELAXATION TIME

To calculate the electron self-energy due to scattering from fluctuations of the exchange field and from localized impurities we utilize the second-order perturbation theory which yields

$$\Sigma^R(\varepsilon,\mathbf{k}) = \int \frac{d^2\mathbf{k}'}{(2\pi)^2}\,\langle \hat{V}_{\mathbf{k}\mathbf{k}'}\,G^{0R}(\varepsilon,\mathbf{k}')\,\hat{V}_{\mathbf{k}'\mathbf{k}}\rangle, \tag{4}$$

with the Green function given by Eq. (3). Since we are interested in the relaxation time of quasiparticles we focus on the imaginary part of self-energy $\mathrm{Im}[\Sigma_R]$ only, i.e., we neglect the real part of self-energy. From Eq. (4) we find

$$\Sigma^R(\varepsilon,\mathbf{k}) = -i\Gamma_0\sigma_0 - i\boldsymbol{\Gamma}\cdot\boldsymbol{\sigma}, \tag{5}$$

where

$$\Gamma_0 = \frac{\pi}{2}\int \frac{d^2\mathbf{k}'}{(2\pi)^2}\,[\langle |V_{\mathbf{k}\mathbf{k}'}|^2\rangle + \mathcal{C}(|\mathbf{k}-\mathbf{k}'|)] \times [\delta(\varepsilon-\varepsilon_{k'}) + \delta(\varepsilon+\varepsilon_{k'})], \tag{6}$$

$$\boldsymbol{\Gamma} = \frac{-\pi}{2\varepsilon}\int \frac{d^2\mathbf{k}'}{(2\pi)^2}\,\mathcal{C}(|\mathbf{k}-\mathbf{k}'|)\,v\mathbf{k}' \times [\delta(\varepsilon-\varepsilon_{k'}) + \delta(\varepsilon+\varepsilon_{k'})]. \tag{7}$$

Upon integrating over the wave vector $\mathbf{k}'$ on the surface of a constant energy, $k = k_1 = |\varepsilon|/v$, we find the solution

$$\Gamma_0 = \frac{k_1}{4v}\langle M^2\rangle\xi^2 e^{-x}\mathcal{I}_0(x) + n_i V_0^2\frac{|\varepsilon|}{4v^2}, \tag{8}$$

$$\boldsymbol{\Gamma} = -\frac{\mathbf{k}}{k}\frac{\langle M^2\rangle}{4\varepsilon}\xi^2 k_1^2 e^{-x}\mathcal{I}_1(x). \tag{9}$$

$\mathcal{I}_0(x)$ and $\mathcal{I}_1(x)$ are the modified Bessel functions of the zeroth and first kind, respectively, and $x = 2\xi^2 k_1^2$. Accordingly, the averaged retarded/advanced Green function in the weak scattering approximation has the form

$$G^{R/A}(\varepsilon,\mathbf{k}) = \frac{\varepsilon\sigma_0 + v\mathbf{k}\cdot\boldsymbol{\sigma}}{(\varepsilon-\varepsilon_k\pm i\gamma_1)(\varepsilon+\varepsilon_k\pm i\gamma_2)}, \tag{10}$$

where

$$\gamma_{1,2} = \Gamma_0 \pm \frac{\mathbf{k}}{k}\cdot\boldsymbol{\Gamma}. \tag{11}$$

The relaxation rates $\gamma_{1,2}$ take the following explicit form:

$$\gamma_{1,2} = \gamma_M + \gamma_0, \tag{12}$$

with

$$\gamma_M = \frac{k_1}{4v}\langle M^2\rangle\xi^2\exp\left(-2\xi^2k_1^2\right) \times \left[\mathcal{I}_0\left(2\xi^2k_1^2\right) + (\varepsilon)\mathcal{I}_1\left(2\xi^2k_1^2\right)\right], \tag{13}$$

$$\gamma_0 = n_i V_0^2\frac{|\varepsilon|}{4v^2}. \tag{14}$$

The expression for the relaxation rate is the same for the negative and the positive energy branches, $\gamma_1 = \gamma_2 \equiv \gamma$, and is fully determined by the intrinsic properties of the topological insulator, i.e., by v_F, k_F, and the two parameters describing the spatial magnetization fluctuations $\langle M^2\rangle$ and ξ, and by the two parameters describing the scalar impurities V_0 and n_i. The electron relaxation time is given by the relation

$$\tau = \frac{\hbar}{2\gamma}. \tag{15}$$

Note, $1/\tau = 1/\tau_M + 1/\tau_0$, according to Eq. (12).

From the above formulas one can see how the random magnetization fluctuations influence the relaxation processes. Generally, one can distinguish two situations. In the first one the magnetization fluctuations follow from the presence of the random magnetic impurities. The impurity scattering potential contains then magnetic and the scalar components. The second situation corresponds to a topological insulator covered by a magnetic insulator. The proximity effect and the interface roughness result in effective spatially fluctuating magnetization which is exchange coupled to the electronic surface states of the topological insulator. In other words, one may assume the relaxation times τ_M and τ_0 are either correlated or independent. In the following we will treat them as independent parameters.

The correlation length of spatial fluctuations of the magnetization may be temperature dependent, $\xi = \xi(T)$. Such a dependence is a consequence of the fact that the fluctuations of magnetization (fluctuations of magnetic moments of adatoms) depend in general on the temperature. In such a case, one can introduce the temperature dependence of the correlation length by the following phenomenological formula [40]:

$$\xi = \xi_0\left[1 - \exp\left(-\frac{\Delta}{k_B T}\right)\right], \tag{16}$$

where $\xi_0 = \xi(T = 0)$ and Δ is the energy scale for magnetic interaction between the impurities.

Figure 1 shows behavior of the relaxation time with energy and temperature for indicated parameters of the magnetic fluctuations ($\langle M^2\rangle$, Δ, ξ_0), and for a constant impurity scattering potential $n_i V_0^2$. Figures 1(a) and 1(b) present the relaxation time as a function of energy ε for different values of $\langle M^2\rangle$ [Fig. 1(a)] and different values of the correlation length ξ_0 [Fig. 1(b)]. The curves corresponding there to $\langle M^2\rangle = 0$ describe the relaxation time due to random impurities only. This relaxation time decreases with energy as $1/\varepsilon$ [see Eq. (14)]. Note, the energy dependence is shown only for positive values of ε.

The other curves in Figs. 1(a) and 1(b) present modification of the relaxation time due to magnetic fluctuations. One can distinguish the range of the parameters for which the relaxation time is strongly modified compared to a system without random magnetization. This modification is determined by the two factors in the correlation function: ξ^2 and $\exp(-q^2\xi^2)$. The former factor reduces the scattering rate due to magnetic fluctuations γ_M for small values of ξ, while the second one reduces the scattering rate for large values of ξ, $\xi \gg (1/q)$, i.e., for the correlation length much longer than the electron wavelength λ (the latter is determined by the Fermi energy μ). For sufficiently high energies, the magnetic fluctuations play a minor role in the relaxation processes and τ is determined mainly by the scattering on scalar potential due to impurities.

Temperature dependence of the relaxation time is shown in Figs. 1(c)–1(f) for indicted parameters of magnetic fluctuations and for low [Figs. 1(c) and 1(d)] and high [Figs. 1(e) and 1(f)] energy. This temperature dependence is due to the decrease of the correlation length with increasing temperature according to Eq. (16). The relaxation time due to scattering on impurities only ($\langle M^2\rangle = 0$) is roughly independent of temperature, see Fig. 1. The situation is different for $\langle M^2\rangle > 0$. For the zero-temperature values of the correlation length

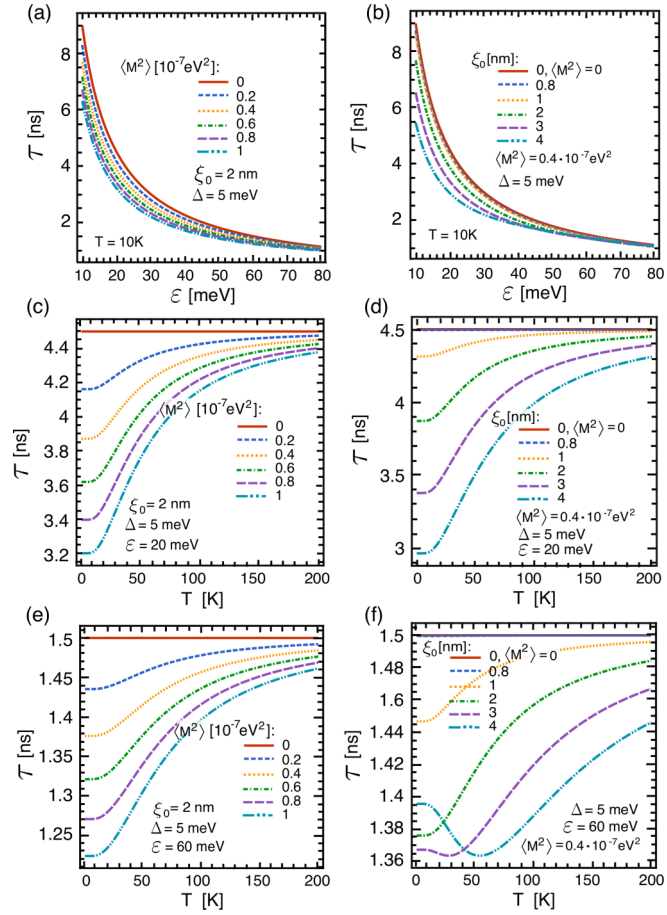

FIG. 1. Relaxation time τ as a function of energy (a) and (b) and as a function of temperature (c)–(f) for indicated values of $\langle M^2\rangle$, correlation length ξ_0, and the parameter Δ. (c) and (d) and (e) and (f) The relaxation time for the low and high energy. The curves corresponding to $\langle M^2\rangle = 0$ present relaxation time due to scattering on impurities only. All curves are for the Fermi velocity $v_F = 3.8 \times 10^5$ m/s and $n_i V_0^2 = 9.14 \times 10^{-25}$ eV^2 m^2.

ξ_0 assumed in Fig. 1, the fluctuations for a fixed chemical potential change character with increasing temperature from the long range ($\xi \gg \lambda$) to short range ($\xi \ll \lambda$). Accordingly, a minimum of the relaxation may be observed at a certain temperature between these two regimes, as clearly visible in Fig. 1(f).

IV. VERTEX FUNCTION AND CONDUCTIVITY

To determine the electrical conductivity, the vertex function is required. Thus, we write the DC current density within the Kubo formalism [41] as

$$j_x = -\frac{evE_x}{2\pi}\,\mathrm{Tr}\int\frac{d^2\mathbf{k}}{(2\pi)^2}\int d\varepsilon\, f'(\varepsilon) J_x(\mathbf{k})\, G^R_{\mathbf{k}}(\varepsilon)\,\sigma_x\, G^A_{\mathbf{k}}(\varepsilon), \tag{17}$$

where $f(\varepsilon)$ is the Fermi-Dirac distribution function, and J_x is the renormalized current density vertex function. Note, in the above formula we have omitted the terms proportional to $G^A G^A$ and $G^R G^R$. Such terms in the problems that can be treated perturbatively (like in our case) give a small correction

to the main term determined by the product $G^R G^A$ (see the Appendix for more details).

The renormalized current vertex in the ladder approximation can be calculated from the self-consistent equation

$$\mathbf{J}(\mathbf{k}) = \hat{\mathbf{j}} + n_i V_0^2 \int \frac{d^2\mathbf{k}'}{(2\pi)^2} G^A(\varepsilon, \mathbf{k}')\, \mathbf{J}(\mathbf{k}') G^R(\varepsilon, \mathbf{k}') + \int \frac{d^2\mathbf{k}'}{(2\pi)^2} \mathcal{C}(\mathbf{k}-\mathbf{k}')\sigma_z\, G^A(\varepsilon, \mathbf{k}')\, \mathbf{J}(\mathbf{k}') G^R(\varepsilon, \mathbf{k}')\sigma_z, \tag{18}$$

where $\hat{\mathbf{j}} = ev\boldsymbol{\sigma}/\hbar$ is the operator of electrical current density. Generally, the current density vertex function can be written in the form

$$\mathbf{J}(\mathbf{k}) = \frac{ev}{\hbar}\,(\mathbf{k}\, g_{0\mathbf{k}}\sigma_0 + g_{1\mathbf{k}}\boldsymbol{\sigma}). \tag{19}$$

Inserting then Eq. (19) into Eq. (18) one finds the solutions for $g_{0\mathbf{k}}$ and $g_{1\mathbf{k}}$ in the following form:

$$g_{0k_1} = \frac{v}{\kappa}\frac{\eta}{\varepsilon}\mathcal{I}_1(x), \tag{20}$$

$$g_{1k_1} = \frac{1}{\kappa}[1 - \eta\mathcal{I}_1(x)], \tag{21}$$

where κ and η are defined as

$$\kappa = 1 - \frac{1}{2}\eta_0 + \frac{\eta}{4}\{3\mathcal{I}_0(x) - 4\mathcal{I}_1(x) + \mathcal{I}_2(x) + \mathcal{I}_1(x)[\mathcal{I}_2(x) - \mathcal{I}_0(x)]\eta\}, \tag{22}$$

$$\eta = \langle M^2\rangle \xi^2 \frac{k_1}{4v\gamma} e^{-2\xi^2 k_1^2}, \tag{23}$$

and $\eta_0 = \gamma_0/\gamma$. Importantly, the renormalized vertex function contains two components. One component [the second term in Eq. (19)] is in fact a simple renormalization of the current density operator $\hat{\mathbf{j}} \to g_{1\mathbf{k}}\hat{\mathbf{j}}$, while the second component is proportional to $\mathbf{k}\sigma_0$. Because of this, one cannot rewrite $\mathbf{J}(\mathbf{k})$ simply in terms of the transport relaxation time $\tau_{\rm tr}$, as it can be done in quasiclassical calculations, where $\hat{\mathbf{j}} \to \hat{\mathbf{j}}\,\tau_{\rm tr}/\tau$. Note also that in the limit $\langle M^2\rangle = 0$ (no magnetic fluctuations) we obtain immediately: $g_{0k_1} = 0$ and $g_{1k_1} = 2$, as it has been derived previously (see, e.g., [29]) for short-range pointlike scalar impurities. Taking into account the explicit form of the current density vertex function, one finds the diagonal conductivity in the form

$$\sigma_{xx} = -\frac{e^2v^2}{2\pi\hbar}\mathrm{Tr}\int\frac{d^2\mathbf{k}}{(2\pi)^2}\int d\varepsilon\, f'(\varepsilon)\big\{k_x g_{0\mathbf{k}} G^R_{\mathbf{k}}(\varepsilon)\,\sigma_x\, G^A_{\mathbf{k}}(\varepsilon) + g_{1\mathbf{k}}\sigma_x G^R_{\mathbf{k}}(\varepsilon)\,\sigma_x\, G^A_{\mathbf{k}}(\varepsilon)\big\}. \tag{24}$$

Upon integrating the above equation over the wave vector $\mathbf{k}$ one can rewrite it as

$$\sigma_{xx} = -\frac{e^2}{8\pi\hbar}\int d\varepsilon f'(\varepsilon)\left[\varepsilon^2\frac{g_{1k_1}}{vk_1\gamma} + \varepsilon\frac{k_1}{\gamma}g_{0k_1}\right]. \tag{25}$$

Taking into account the relation

$$\varepsilon^2\frac{g_{1k_1}}{vk_1\gamma} + \varepsilon\frac{k_1}{\gamma}g_{0k_1} = \frac{vk_1}{\gamma\kappa}, \tag{26}$$

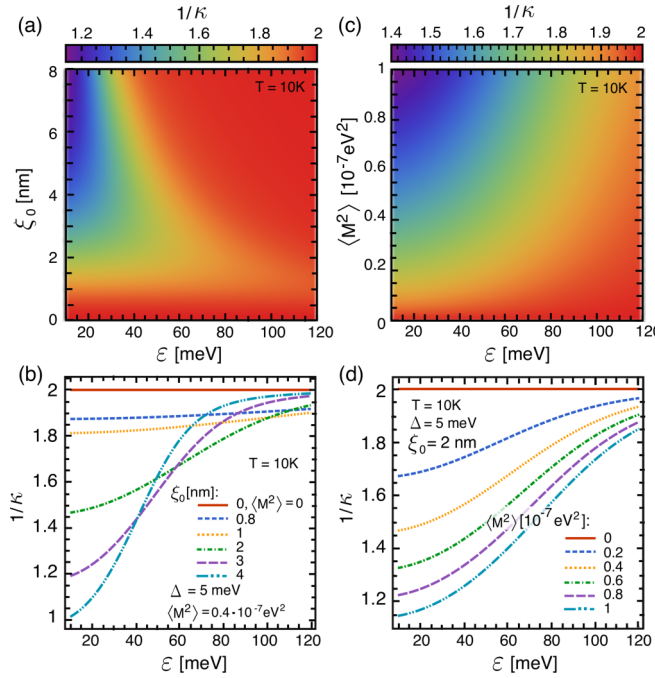

FIG. 2. Parameter $1/\kappa$, describing the vertex correction to conductivity, plotted as a function of energy ε and correlation length ξ_0 for $\Delta = 5$ meV, $\langle M^2\rangle = 0.4\times10^{-7}$ eV^2 (a), and as a function of energy and $\langle M^2\rangle$ for $\Delta = 5$ meV, $\xi_0 = 2$ nm (c). (b) and (d) The corresponding cross sections for indicated values of ξ_0 (b) and $\langle M^2\rangle$ (d). Other parameters, if not indicated, are the same as in Fig. 1.

the conductivity is cast in the following form:

$$\sigma_{xx} = -\frac{e^2}{h}\int d\varepsilon f'(\varepsilon)\frac{|\varepsilon|}{4\gamma\kappa}, \tag{27}$$

where $f'(\varepsilon) = \partial f/\partial\varepsilon$.

As follows from Eqs. (11) and (22), both the relaxation rate γ and the parameter κ depend on energy. The latter parameter describes the influence of vertex correction due to scalar impurity potential and magnetic fluctuations. More specifically, the electrical conductivity is renormalized due to vertex corrections by a factor $1/\kappa$, see Eq. (27). Figures 2(a) and 2(c) present $1/\kappa$ as a function of energy and correlation length ξ_0 (a) and as a function of energy and amplitude of the magnetization fluctuations $\langle M^2\rangle$ (c). The corresponding cross sections are presented in Figs. 2(b) and 2(d). As already mentioned above, the parameter $1/\kappa$ is equal to 2 in the absence of magnetic fluctuations $\langle M^2\rangle = 0$ [see the corresponding curves in Figs. 2(b) and 2(d)]. The magnetic fluctuations reduce the parameter $1/\kappa$ to values lower than 2. This is clearly seen, especially for lower energies, where the relative contribution due to scattering on magnetic fluctuations is remarkable.

The formula (27) is our final result which will be now used for further analysis and discussion of numerical results. The longitudinal conductivity is presented in Fig. 3, where Figs. 3(a) and 3(b) present the conductivity as a function of the chemical potential μ and correlation length ξ_0, and as a function of the chemical potential and $\langle M^2\rangle$, respectively. Both Figs. 3(a) and 3(b) are for the same temperature $T =$ 10 K. The corresponding cross sections for indicated values of

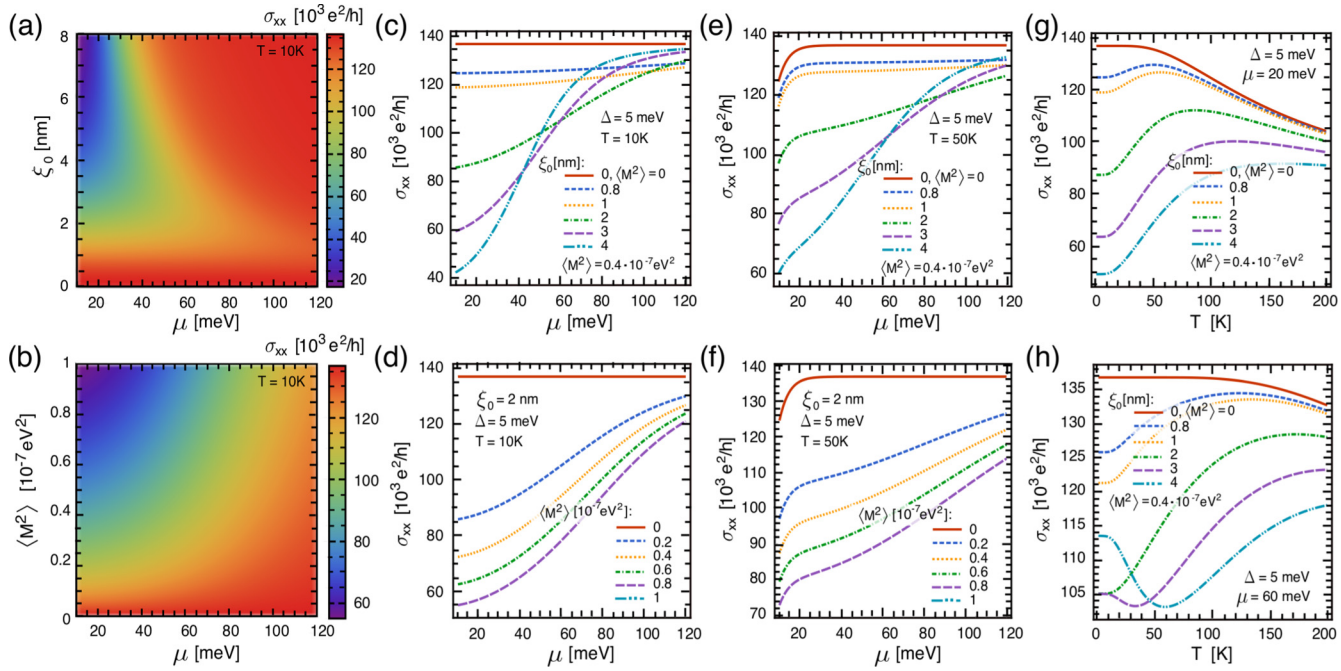

FIG. 3. Electrical conductivity as a function of the chemical potential μ and correlation length ξ_0 for $\Delta = 5$ meV, $\langle M^2\rangle = 0.4 \times 10^{-7}$ eV^2 (a), and as a function of the chemical potential and $\langle M^2\rangle$ for $\Delta = 5$ meV, $\xi_0 = 2$ nm (b). The corresponding cross sections for indicated values of ξ_0 and $\langle M^2\rangle$ are shown in (c) and (d), respectively. The results shown in (a)–(d) are for the temperature $T = 10$ K. (e) and (f) The same as in (c) and (d), except for the temperature which now is $T = 50$ K (e). Temperature dependence of the electrical conductivity is shown explicitly in (g) and (h) for different values of the chemical potential $\mu = 20$ meV (g) and $\mu = 60$ meV (h). Other parameters as in Fig. 1.

ξ_0 and $\langle M^2\rangle$ are shown in Figs. 3(c) and 3(d), respectively. As one can note, the magnetic fluctuations remarkably change the longitudinal conductivity in comparison to the conductivity of surface electrons in a nonmagnetic TI [shown in Figs. 3(c)–3(h) by the curves for $\langle M^2\rangle = 0$]. Note, when $\langle M^2\rangle = 0$, then the conductivity is determined by scattering on impurities and is roughly independent of the chemical potential, see Figs. 3(c) and 3(d). This behavior is a consequence of two facts: (i) the relaxation time decays with increasing the chemical potentials as $1/|\mu|$, and (ii) the carrier density is proportional to the chemical potential $|\mu|$. As a result, the conductivity is then roughly independent of μ. Some deviation from this appear at higher temperatures and low chemical potentials, see Figs. 3(e) and 3(f) which show the same as in Figs. 3(c) and 3(d), except temperature which now is $T =$ 50 K. This is also visible in Figs. 3(g) and 3(h) for higher temperatures. In agreement with our earlier discussion, the conductivity in the presence of magnetic fluctuations grows with increasing chemical potential and tends to the value determined by scattering on impurities. This is clearly seen in Figs. 3(c)–3(f).

Temperature dependence of the electrical conductivity is shown explicitly in Figs. 3(g) and 3(h) for different values of the chemical potential. Interestingly, in the presence of magnetic fluctuations, the conductivity for low values of chemical potential [see Fig. 3(g)] increases with temperature due to the reduction of the correlation length. However, after reaching a maximum, it decreases with a further increase of T. For high temperatures, the conductivity tends to that in the nonmagnetic case due to suppression of the magnetic fluctuations with increasing temperature. For higher chemical potentials, see Fig. 3(h), the temperature dependence is more complex and the conductivity may reach a minimum at a certain temperature and then grow with a further increase in T. This is a consequence of the interplay of both scattering processes contributing to the vertex function and both sources of temperature dependence (Fermi-Dirac distribution and temperature dependence of the correlation length).

V. SUMMARY AND CONCLUSIONS

We studied the impact of correlated fluctuations of magnetization (exchange field) on the transport properties of surface 2D electrons in topological insulators. The fluctuations have been described by their amplitude $\sqrt{\langle M^2\rangle}$ and correlation length ξ. We have also taken into account the reduction of the correlation length with increasing temperature, following a simple phenomenological formula. The description is based on a perturbative approach. Thus, the amplitude of the fluctuations as well as the appropriate correlation length cannot be arbitrarily large. To infer the electrical conductivity we determined at first the relaxation rate and then the appropriate current density vertex function. The latter turned out to have a significant influence on the conductivity. The relaxation time and electrical conductivity were calculated assuming additional scattering on impurities with pointlike scalar scattering potential. Both scattering on magnetization fluctuations and scattering on nonmagnetic impurities were taken into account on equal footing in the calculations of both the relaxation time and the vertex function.

The conductivity is remarkably reduced by scattering on magnetization fluctuations in comparison to that in the absence of such fluctuations—especially at higher Fermi energies, where scattering on impurities plays a dominant role. The temperature dependence of transport properties was also calculated and discussed. The temperature dependence of the conductivity follows not only from the Fermi distribution function, but also from the temperature dependence of the correlation length of the magnetization fluctuations. This results, for a specific range of parameters, in an increase of the longitudinal conductivity with temperature. A similar behavior of the longitudinal conductivity with the temperature has been observed recently for surface states of TI in experiments with Mn-doped $Bi_2Te_{3-y}Se_y$ [42], Cr-doped $(Bi_xSb_{1-x})_2Te_3$ [43].

ACKNOWLEDGMENTS

This work is supported by the National Science Center in Poland under Grant No. DEC-2017/27/B/ST3/02881. A.D. acknowledges support by DFG through SFB TRR227.

APPENDIX: CONTRIBUTION OF TERMS WITH G^RG^R AND G^AG^A

Let us estimate the contribution of terms with G^RG^R and G^AG^A to the conductivity

$$\delta\sigma_{xx}^{RR+AA} = -\frac{e^2v^2}{2\pi\hbar}\mathrm{Tr}\int\frac{d^2\mathbf{k}}{(2\pi)^2}\int d\varepsilon\, f'(\varepsilon)\,\sigma_x\big[G^R_{\mathbf{k}}(\varepsilon)\,\sigma_x\,G^R_{\mathbf{k}}(\varepsilon)+G^A_{\mathbf{k}}(\varepsilon)\,\sigma_x\,G^A_{\mathbf{k}}(\varepsilon)\big]. \tag{A1}$$

Substituting (10) to (A1) and calculating the trace we get

$$\delta\sigma_{xx}^{RR} = -\frac{e^2}{4\pi\hbar}\int\frac{d^2\mathbf{k}}{(2\pi)^2}\int d\varepsilon\, f'(\varepsilon)\,\frac{\varepsilon^2}{k^2}\left(\frac{1}{\varepsilon-vk+i\gamma_1}-\frac{1}{\varepsilon+vk+i\gamma_2}\right)\left(\frac{1}{\varepsilon-vk+i\gamma_1}-\frac{1}{\varepsilon+vk+i\gamma_2}\right) \tag{A2}$$

$$\simeq -\frac{e^2}{8\pi^2\hbar v^2}\int\varepsilon^2 d\varepsilon\, f'(\varepsilon)\int_0^\infty\frac{dk}{k}\left[\frac{1}{(k-k_1)^2}+\frac{1}{(k+k_1)^2}+\frac{2}{(k-k_1)(k+k_1)}\right], \tag{A3}$$

where $k_1 = |\varepsilon|/v$.

Then after calculating the integrals over k we obtain

$$\delta\sigma_{xx}^{RR} = \frac{e^2}{4\pi^2\hbar v^2}\int\varepsilon^2 d\varepsilon\, f'(\varepsilon)\,\frac{1}{k_1^2}\,\frac{k^2}{k^2-k_1^2}\bigg|_0^\infty \simeq -\frac{e^2}{4\pi^2\hbar}. \tag{A4}$$

Since the real parts of contributions coming from G^RG^R and G^AG^A are equal we obtain

$$\delta\sigma_{xx}^{RR+AA} \simeq -\frac{e^2}{2\pi^2\hbar}. \tag{A5}$$

This contribution is small comparing to (27) since $\gamma \ll \mu$ and $\kappa \sim 1$. In other words, the correction from terms with G^RG^R and G^AG^A is small if $\mu\tau_{tr}/\hbar \gg 1$.

[1] M. Z. Hasan and C. L. Kane, Colloquium: Topological insulator, Rev. Mod. Phys. **82**, 3045 (2010).
[2] X.-L. Qi and S.-C. Zhang, Topological insulators and superconductors, Rev. Mod. Phys. **83**, 1057 (2011).
[3] Y. Xia, D. Qian, D. Hsieh, L. Wray, A. Pal, H. Lin, A. Bansil, D. Grauer, Y. S. Hor, R. J. Cava, and M. Z. Hasan, Observation of a large-gap topological-insulator class with a single Dirac cone on the surface, Nat. Phys. **5**, 398 (2009).
[4] D. Hsieh, Y. Xia, D. Qian, L. Wray, J. H. Dil, F. Meier, J. Osterwalder, L. Patthey, J. G. Checkelsky, N. P. Ong, A. V. Fedorov, H. Lin, A. Bansil, D. Grauer, Y. S. Hor, R. J. Cava, and M. Z. Hasan, A tunable topological insulator in the spin helical Dirac transport regime, Nature (London) **460**, 1101 (2009).
[5] H.-Z. Lu, W.-Yu. Shan, W. Yao, Q. Niu, and S.-Q. Shen, Massive Dirac fermions and spin physics in an ultrathin film of topological insulator, Phys. Rev. B **81**, 115407 (2010).
[6] M. Konig, S. Wiedmann, C. Brune, A. Roth, H. Buhmann, L. W. Molenkamp, X.-L. Qi, and S.-C. Zhang, Quantum spin Hall insulator state in HgTe quantum wells, Science **318**, 766 (2007).
[7] Y. Xu, I. Miotowski, and Y. P. Chen, Quantum transport of two-species Dirac fermions in dual-gated three-dimensional topological insulators, Nat. Commun. **7**, 11434 (2016).
[8] R. S. Akzyanov and A. L. Rakhmanov, Surface charge conductivity of a topological insulator in a magnetic field: The effect of hexagonal warping, Phys. Rev. B **97**, 075421 (2018).
[9] R. S. Akzyanov and A. L. Rakhmanov, Bulk and surface spin conductivity in topological insulators with hexagonal warping, Phys. Rev. B **99**, 045436 (2019).
[10] P. He, S. S.-L. Zhang, D. Zhu, Y. Liu, Y. Wang, J. Yu, G. Vignale, and H. Yang, Bilinear magnetoelectric resistance as a probe of three-dimensional spin texture in topological surface states, Nat. Phys. **14**, 495 (2018).
[11] Y. Lv, J. Kally, D. Zhang, J. S. Lee, M. Jamali, N. Samarth, and J.-P. Wang, Unidirectional spin-Hall and Rashba-Edelstein

magnetoresistance in topological insulator-ferromagnet layer heterostructures, Nat. Commun. **9**, 111 (2018).

[12] A. Soumyanarayanan, N. Reyren, A. Fert, and Ch. Panagopoulos, Emergent phenomena induced by spin-orbit coupling at surfaces and interfaces, Nature (London) **539**, 509 (2016).

[13] H. Zhang, C.-X. Liu, X.-L. Qi, X. Dai, Z. Fang, and S.-C. Zhang, Topological insulators in Bi_2Se_3, Bi_2Te_3 and Sb_2Te_3 with a single Dirac cone on the surface, Nat. Phys. **5**, 438 (2009).

[14] X. Kou, L. He, M. Lang, Y. Fan, K. Wong, Y. Jiang, T. Nie, W. Jiamg, P. Upadhyaya *et al.*, Manipulating surface-related ferromagnetism in modulation-doped topological insulators, Nano Lett. **13**, 4587 (2013).

[15] Y. Fan, P. Upadhyaya, X. Kou, M. Lang, S. Takei, Z. Wang, J. Tang, L. He, L.-T. Chang, M. Montazeri *et al.*, Magnetization switching through giant spin-orbit torque in a magnetically doped topological insulator heterostructure, Nat. Mater. **13**, 699 (2014).

[16] H. Wang, J. Kally, J. S. Lee, T. Liu, H. Chang, D. R. Hickey, K. A. Mkhoyan, M. Wu, A. Richardella, and N. Samarth, Surface-State-Dominated Spin-Charge Current Conversion in Topological-Insulator-Ferromagnetic-Insulator Heterostructures, Phys. Rev. Lett. **117**, 076601 (2016).

[17] Y.-Y. Zhang, X.-R. Wang, and X. C. Xie, Three-dimensional topological insulator in a magnetic field: Chiral side surface states and quantized Hall conductance, J. Phys.: Condens. Matter **24**, 015004 (2012).

[18] Y. Xu, I. Miotowski, C. Liu, J. Tian, H. Nam, N. Alidoust, J. Hu, C.-K. Shih, M. Z. Hasan, and Y. P. Chen, Observation of topological surface state quantum Hall effect in an intrinsic three-dimensional topological insulator, Nat. Phys. **10**, 956 (2014).

[19] T. Morimoto, A. Furusaki, and N. Nagaosa, Topological magnetoelectric effects in thin films of topological insulators, Phys. Rev. B **92**, 085113 (2015).

[20] M. Fähnle and H. Kronmüller, The influence of spatially random magnetostatic, magnetocrystalline, magnetostrictive and exchange fluctuations on the law of approach to ferromagnetic saturation of amorphous ferromagnets, J. Magn. Magnet. Mater. **8**, 149 (1978).

[21] J. D. Bernal, A geometrical approach to the structure of liquids, Nature (London) **183**, 141 (1959).

[22] J. D. Bernal, Geometry of the structure of monatomic liquids, Nature (London) **185**, 68 (1960).

[23] S. J. Bending, K. von Klitzing, and K. Ploog, Two-dimensional electron gas as a flux detector for a type-II superconducting film, Phys. Rev. B **42**, 9859 (1990).

[24] S. J. Bending, K. von Klitzing, and K. Ploog, Weak Localization in a Distribution of Magnetic Flux Tubes, Phys. Rev. Lett. **65**, 1060 (1990).

[25] A. K. Geim, S. J. Bending, and I. V. Grigorieva, Asymmetric Scattering and Diffraction of Two-Dimensional Electrons at Quantized Tubes of Magnetic Flux, Phys. Rev. Lett. **69**, 2252 (1992).

[26] A. K. Geim, S. J. Bending, I. V. Grigorieva, and M. G. Blamire, Ballistic two-dimensional electrons in a random magnetic field, Phys. Rev. B **49**, 5749(R) (1994).

[27] F. B. Mancoff, R. M. Clarke, C. M. Marcus, S. C. Zhang, K. Campman, and A. C. Gossard, Magnetotransport of a two-dimensional electron gas in a spatially random magnetic field, Phys. Rev. B **51**, 13269 (1995).

[28] F. B. Mancoff, L. J. Zielinski, C. M. Marcus, K. Campman, and A. C. Gossard, Shubnikov–de Haas oscillations in a two-dimensional electron gas in a spatially random magnetic field, Phys. Rev. B **53**, R7599(R) (1996).

[29] T. Chiba, S. Takahashi, and G. E. W. Bauer, Magnetic-proximity-induced magnetoresistance on topological insulators, Phys. Rev. B **95**, 094428 (2017).

[30] P. M. Ostrovsky, I. V. Gornyi, and A. D. Mirlin, Electron transport in disordered graphene, Phys. Rev. B **74**, 235443 (2006).

[31] A. Schuessler, P. M. Ostrovsky, I. V. Gornyi, and A. D. Mirlin, Analytic theory of ballistic transport in disordered graphene, Phys. Rev. B **79**, 075405 (2009).

[32] A. W. W. Ludwig, M. P. A. Fisher, R. Shankar, and G. Grinstein, Integer quantum Hall transition: An alternative approach and exact results, Phys. Rev. B **50**, 7526 (1994).

[33] S. Wozny, K. Vyborny, W. Belzig, and S. I. Erlingsson, Gap formation in helical edge states with magnetic impurities, Phys. Rev. B **98**, 165423 (2018).

[34] L. Chotorlishvili, A. Ernst, V. K. Dugaev, A. Komnik, M. G. Verginiory, E. V. Chulkov, and J. Berakdar, Magnetic fluctuations in topological insulators with ordered magnetic adatoms: Cr on Bi_2Se_3 from first principles, Phys. Rev. B **89**, 075103 (2014).

[35] A. Pieper and H. Fehske, Topological insulators in random potentials, Phys. Rev. B **93**, 035123 (2016).

[36] Y. Xing, F. Xu, K. T. Cheung, Q.-F. Sun, J. Wang, and Y. Yao, Geometric effect on quantum anomalous Hall states in magnetic topological insulators, New J. Phys. **20**, 043011 (2018).

[37] H. M. Hurst, D. K. Efimkin, and V. Galitski, Transport of Dirac electrons in a random magnetic field in topological heterostructures, Phys. Rev. B **93**, 245111 (2016).

[38] M. M. Glazov, E. Ya. Sherman, and V. K. Dugaev, Two-dimensional electron gas with spin-orbit coupling disorder, Physica E **42**, 2157 (2010).

[39] S. Kudła, A. Dyrdał, V. K. Dugaev, E. Ya. Sherman, and J. Barnaś, Charge and spin conductivity of a two-dimensional electron gas with a random Rashba interaction, Phys. Rev. B **97**, 245307 (2018).

[40] The exponential form of this formula is chosen as the probability of fluctuation is usually determined by the exponent [see, e.g., L. D. Landau and E. M. Lifshitz, *Statistical Physics, Part 1* (Pergamon, New York, 1980), Chap. XIV].

[41] G. D. Mahan, *Many-Particle Physics* (Springer, New York, 2000).

[42] J. G. Checkelsky, J. Ye, Y. Onose, Y. Iwasa, and Y. Tokura, Dirac-fermion-mediated ferromagnetism in a topological insulator, Nat. Phys. **8**, 729 (2012).

[43] C.-Z. Chang, J. Zhang, M. Liu, Z. Zhang, X. Feng, K. Li, L.-L. Wang, X. Chen, Xi Dai, Z. Fang, X.-L. Qi, S.-C. Zhang, Y. Wang, K. He, X.-C. Ma, and Q.-K. Xue, Thin films of magnetically doped topological insulator with carrier-independent long-range ferromagnetic order, Adv. Mater. **25**, 1065 (2013).